

Arbitrary Pattern Formation on Infinite Regular Tessellation Graphs^{*}

Serafino Cicerone¹, Alessia Di Fonso¹, Gabriele Di Stefano¹, Alfredo Navarra²

¹ Dipartimento di Ingegneria e Scienze dell'Informazione e Matematica, Università degli Studi dell'Aquila, I-67100 L'Aquila, Italy. serafino.cicerone@univaq.it, alessia.difonso@graduate.univaq.it, gabriele.distefano@univaq.it

² Dipartimento di Matematica e Informatica, Università degli Studi di Perugia I-06123 Perugia, Italy. alfredo.navarra@unipg.it

Abstract. Given a set R of robots, each one located at different vertices of an infinite regular tessellation graph, we aim to explore the *Arbitrary Pattern Formation (APF)* problem. Given a multiset F of grid vertices such that $|R| = |F|$, *APF* asks for a distributed algorithm that moves robots so as to reach a configuration similar to F . Similarity means that robots must be disposed as F regardless of translations, rotations, reflections.

So far, as possible graph discretizing the Euclidean plane only the standard square grid has been considered in the context of the classical *Look-Compute-Move* model. However, it is natural to consider also the other regular tessellation graphs, that are triangular and hexagonal grids.

We provide a resolution algorithm for *APF* when the initial configuration is asymmetric and the considered topology is any regular tessellation graph.

Keywords: Distributed Algorithms · Mobile Robots · Asynchrony · Pattern Formation · Graphs

1 Introduction

In this paper, we consider the *Arbitrary Pattern Formation (APF)* task by means of a swarm of very weak - in terms of capabilities - robots moving on graphs. Initially, each robot occupies a different vertex of the graph. This task calls for a distributed algorithm that allows a set of autonomous mobile robots *to form any specific but arbitrary geometric pattern given as input*. The pattern formation task is one of the basic primitives extensively studied in the context of robot-based computing systems. Whether or not a mobile robot system can solve a given problem typically depends on the capabilities one assumes for robots. A common approach in distributed computing is to detect the minimal capabilities that are necessary so as robots can perform basic tasks. The rationale behind this approach is twofold: it is theoretically interesting to answer the minimality question; the weaker the model assumed to solve a task, the wider its applicability, including more powerful robots prone to faults.

1.1 Robots' model

In this paper, robots are considered to be:

- *Anonymous*: no unique identifiers;

^{*} The work has been supported in part by the Italian National Group for Scientific Computation (GNCS-INdAM).

- *Autonomous*: no centralized control;
- *Dimensionless*: no occupancy constraints, no volume, modeled as entities located on vertices of a graph;
- *Oblivious*: no memory of past events;
- *Homogeneous*: they all execute the same *deterministic*³ algorithm;
- *Silent*: no means of direct communication;
- *Disoriented*: no common coordinate system, no common left-right orientation;

Each robot in the system has sensory capabilities allowing it to determine the location of other robots in the graph, relative to its own location. Each robot refers in fact to a *Local Coordinate System* (LCS) that might be different from robot to robot. Each robot follows an identical algorithm that is preprogrammed into the robot. The behavior of each robot can be described according to the sequence of four states: **Wait**, **Look**, **Compute**, and **Move**. Such states form a computational cycle (or briefly a cycle) of a robot.

1. **Wait**. The robot is idle. A robot cannot stay indefinitely idle.
2. **Look**. The robot observes the environment by activating its sensors which will return a snapshot of the positions of all other robots with respect to its LCS. Each robot is viewed as a point. Hence, the result of the snapshot (i.e., of the observation) is just a set of coordinates in its LCS.
3. **Compute**. The robot performs a local computation according to a deterministic algorithm \mathcal{A} (we also say that the robot executes \mathcal{A}). The algorithm is the same for all robots, and the result of the **Compute** phase is a destination point along with a path to reach it.
4. **Move**. If the destination point is the current vertex where r resides, r performs a *nil* movement (i.e., it does not move); otherwise it moves to the adjacent vertex selected along the computed path.

When a robot is in **Wait** we say it is *inactive*, otherwise it is *active*. In the literature, the computational cycle is simply referred to as the **Look-Compute-Move** (LCM) cycle, as during the **Wait** phase a robot is inactive. Initially robots are inactive, but once the execution of an algorithm \mathcal{A} starts - unless differently specified - there is no instruction to stop it, i.e., to prevent robots to enter their LCM cycles. Then, the *termination* property for \mathcal{A} can be stated as follows: once robots have reached the required goal by means of \mathcal{A} , from there on robots can perform only the *nil* movement.

During the **Look** phase, robots can perceive *multiplicities*, that is whether a same point is occupied by more than one robot. The multiplicity detection capability might be *local* or *global*, depending whether the multiplicity is detected only by robots composing the multiplicity or by any robot performing the **Look** phase, respectively. Moreover, the multiplicity detection can be *weak* or *strong*, depending whether a robot can detect only the presence of a multiplicity or if it perceives the exact number of robots composing the multiplicity, respectively. In this work we assume that each robot is endowed with the global strong multiplicity detection.

Concerning the movements, in the graph environment moves are always considered as instantaneous. This results in always perceiving robots on vertices and never on edges during **Look** phases. Hence, robots cannot be seen while moving, but only at the moment they may start moving or when they arrived. The rationale behind this assumption is that the graph may model a communication network, whereas robots model software agents.

We assume that cycles are performed according to the weakest Asynchronous scheduler (ASYNC) (cf. [1,6,8,9,14,19,20]): the robots are activated independently, and the duration of each phase is finite

³ No randomization features are allowed.

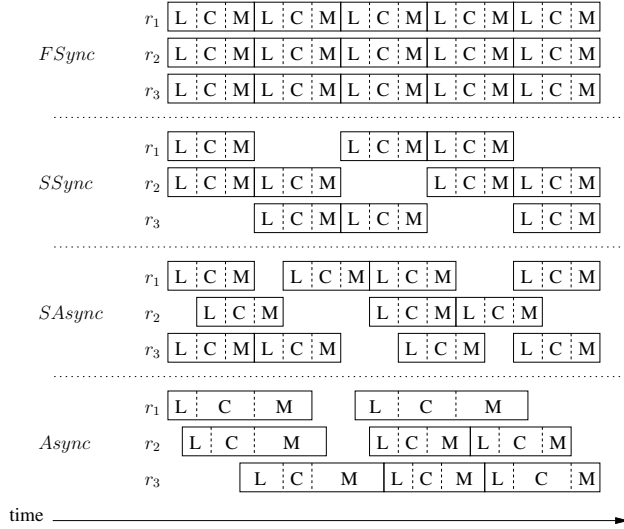


Fig. 1. The execution model of computational cycles for each of *FSync*, *SSync*, *SASync*, and *Async* robots. The inactivity of robots is implicitly represented by empty time periods.

but unpredictable (the activation of each robot can be thought of as decided by the adversary). As a result, robots do not have a common notion of time. Moreover, according to the definition of the *Look* phase, a robot does not perceive whether other robots are moving or not. Hence, robots may move based on outdated perceptions. In fact, due to asynchrony, by the time a robot takes a snapshot of the configuration, this might have drastically changed once the robot starts moving. The scheduler determining the cycles timing is assumed to be fair, that is, each robot becomes active and performs its cycle within finite time and infinitely often. Figure 1 compares the *ASync* scheduler with the other scheduler proposed in the literature. In the figure, the *Wait* state is implicitly represented by the time while a robot is inactive. In particular, it shows that in the Fully-synchronous (*FSync*) scheduler all robots are always active, and the activation phase can be logically divided into global rounds: for all $i \geq 1$, all robots start the i -th LCM cycle simultaneously and synchronously execute each phase.

The Semi-synchronous (*SSync*, cf. [23,24,25]) scheduler coincides with the *FSync* model, with the only difference that some robots may not start the i -th LCM cycle for some i (some of the robots might be in the *Wait* state), but all of those who have started the i -th cycle synchronously execute each phase.

The Semi-asynchronous (*SASync*, cf. [7]) still maintains a sort of synchronous behavior as each phase lasts the same amount of time, but robots can start their LCM cycles at different times. It follows that while a robot is performing a *Look* phase, other active robots might be performing the *Compute* or the *Move* phases.

Clearly, the four synchronization schedulers induce the following hierarchy (see, e.g. [7,13,15]): *FSync* robots are more powerful (i.e. they can solve more tasks) than *SSync* robots, that in turn are more powerful than *SASync* robots, that in turn are more powerful than *ASync* robots. This simply follows by observing that the adversary can control more parameters in *ASync* than in *SASync*, and it controls more parameters in *SASync* than in *SSync* and *FSync*. In other words, protocols designed

for ASYNC robots also work for SASYNC, SSYNC and FSYNC robots. Contrary, any impossibility result stated for FSYNC robots also holds for SSYNC, SASYNC and ASYNC robots.

In the ASYNC scheduler, the activations of the robots determine specific ordered time instants. Let $C(t)$ be the configuration observed by some robots at time t during their Look phase, and let $\{t_i : i = 0, 1, \dots\}$, with $t_i < t_{i+1}$, be the set of all time instances at which at least one robot takes the snapshot $C(t_i)$. Since the information relevant for the computing phase of each robot is the order in which the different snapshots occur and not the exact time in which each snapshot is taken, then without loss of generality we can assume $t_i = i$ for all $i = 0, 1, \dots$. Then, an *execution* of an algorithm \mathcal{A} from an initial configuration C is a sequence of configurations $\mathbb{E} : C(0), C(1), \dots$, where $C(0) = C$ and $C(t+1)$ is obtained from $C(t)$ by moving some robot according to the result of the **Compute** phase as implemented by \mathcal{A} . Notice that this definition of execution works also for the other schedulers. Moreover, given an algorithm \mathcal{A} , in ASYNC (but also in SASYNC and SASYNC) there exists more than one execution from $C(0)$ depending on the activation of the robots (which depends on the adversary).

1.2 Previous work

For robots moving on the Euclidean plane, a restricted version of *APF* has been first solved in [17]. In fact, the proposed algorithm requires at least $n \geq 4$ asynchronous robots endowed with chirality, that is robots share a common handedness. Moreover, the possible patterns exclude the possibility to form multiplicities. The answer to this restricted setting for *APF* provided a nice characterization of the problem that was shown to be equivalent to Leader Election within the same set of assumptions. In particular, the configurations from which the proposed algorithm could output any pattern (without multiplicities) are the so-called *leader configurations*. These are configurations of robots (including some symmetric ones) from which it is possible to elect a leader. Attempts to remove those restrictions can be found in [4,26], but randomization techniques are used. In [8], instead *APF* has been solved by means of a deterministic algorithm, without chirality and allowing multiplicities. Further investigations of *APF* in the Euclidean plane referring to slightly different models can be found in [3,18]. It is worth mentioning that when multiplicities are allowed for the patterns, the degenerate case of point formation (aka *Gathering*) is included in *APF*. Actually, the gathering task has been fully characterized in [11]. It constitutes a very special case that deserves main attention.

For robots moving on graphs, and in particular on an infinite square grid, *APF* has been recently addressed in [2]. The initial configuration is assumed to be asymmetric and still the allowed patterns do not contain multiplicities. Hence, the considered *APF*, so far does not include gathering. Gathering on infinite or finite square grids has been fully characterized in [12,16], also considering the minimization of the overall travelled distances.

1.3 Our results

Our investigation for *APF* on graphs has started by considering square grids allowing also multiplicities in the patterns. Then we realized that a natural extension of the problem is to consider any regular tessellation graph as discretization of the Euclidean plane, that is also hexagonal and triangular grids deserve investigation. In particular, the latter can be considered as the most general topology in terms of possible symmetries and trajectories. In this paper, we address the resolution of *APF*, including multiplicities, on all the three regular tessellations by providing a unique algorithm. The algorithm is first described in details with respect to the triangular grid, when the initial configuration is asymmetric. We follow a formal design and analysis to provide our algorithm, along with

the correctness proof. To this aim, we used the design methodology proposed in [10]. Furthermore we revisit the algorithm with respect to both the square and the hexagonal grids, pointing out any possible deviations required with respect to the specific topology.

1.4 Outline

This paper is organized as follows. Next section first formally defines the addressed problem and then it introduces the notation used by the provided algorithm called \mathcal{A}_{form} . Section 3 provides a high-level description of \mathcal{A}_{form} designed by also remarking the strategy underlying the algorithm. Section 4 formalizes the algorithm and provides the correctness. Since all the details are given with respect to the triangular grid, in Section 5 we revisit the algorithm with respect to both the square and the hexagonal grids. Section 6 concludes the paper by highlighting some final remarks.

2 Problem definition and basic notation

The topology where robots are placed on is represented by a simple, undirected, and connected graph $G = (V, E)$, with vertex set V and edge set E . A function $\lambda : V \rightarrow \mathbb{N}$ represents the number of robots on each vertex of G , and we call $C = (G, \lambda)$ a *configuration* whenever $\sum_{v \in V} \lambda(v)$ is bounded and greater than zero. A vertex $v \in V$ such that $\lambda(v) > 0$ is said *occupied*, *unoccupied* otherwise. A *multiplicity* occurs in any vertex $v \in V$ such that $\lambda(v) > 1$.

2.1 Configurations on tessellation graphs

In this work we consider G as an infinite graph generated by a *plane tessellation*. A tessellation is a tiling of a plane with polygons without overlapping. A *regular tessellation* is a tessellation which is formed by just one kind of regular polygons of side length 1 and in which the corners of polygons are identically arranged. According to [21], there are only three regular tessellations, and they are generated by squares, equilateral triangles or regular hexagons (see Fig. 2). An infinite lattice of a regular tessellation is a lattice formed by taking the vertices of the regular polygons in the tessellation as the points of the lattice. A graph G is induced by the point set S if the vertices of G are the points in S and its edges connect vertices that are distance 1 apart. A *tessellation graph* of a regular tessellation is the infinite graph embedded into the Euclidean plane induced by the infinite lattice formed by that tessellation [22]. We denote by G_S (G_T and G_H , resp.) the tessellation graphs induced by the regular tessellations generated by squares (equilateral triangles and regular hexagons, resp.). In this work we consider configurations $C = (G, \lambda)$ where $G \in \{G_S, G_T, G_H\}$.

Definition 1. *Given a graph $G \in \{G_S, G_T, G_H\}$, any line parallel to a subset of edges of G is called a canonical direction. The smallest angle formed by the available canonical directions is called the canonical angle.*

According to Definition 1, in G_S there are just two canonical directions and the canonical angle is of 90° . In both G_T and G_H there are three canonical directions and the canonical angle is of 60° .

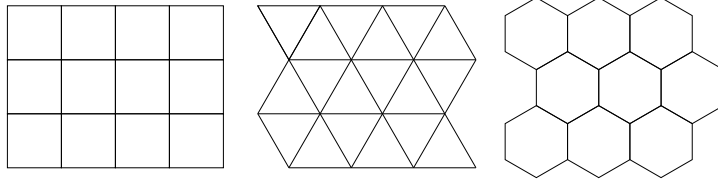


Fig. 2. Part of regular plane tessellations.

2.2 Configuration automorphisms and symmetries

Two undirected graphs $G = (V, E)$ and $G' = (V', E')$ are *isomorphic* if there is a bijection φ from V to V' such that $\{u, v\} \in E$ if and only if $\{\varphi(u), \varphi(v)\} \in E'$. An *automorphism* on a graph G is an isomorphism from G to itself, that is a permutation of the vertices of G that maps edges to edges and non-edges to non-edges. The set of all automorphisms of G , under the composition operation, forms a group called *automorphism group* of G and denoted by $\text{Aut}(G)$. If $|\text{Aut}(G)| = 1$, that is G admits only the identity automorphism, then G is said *asymmetric*, otherwise it is said *symmetric*. Two distinct vertices $u, v \in V$ are *equivalent* if there exists an automorphism $\varphi \in \text{Aut}(G)$ such that $\varphi(u) = v$.

The concept of graph automorphism can be extended to configurations in a natural way: (1) two configurations $C = (G, \lambda)$ and $C' = (G', \lambda')$ are isomorphic if G and G' are isomorphic via an automorphism $\varphi \in \text{Aut}(G)$ and $\lambda(v) = \lambda'(\varphi(v))$ for each vertex v in G ; (2) an automorphism of a configuration $C = (G, \lambda)$ is an isomorphism from C to itself, and (3) the set of all automorphisms of C forms a group under the composition operation that we call automorphism group of C and denote as $\text{Aut}(C)$. Moreover, if $|\text{Aut}(C)| = 1$ we say that C is *asymmetric*, otherwise it is *symmetric*. Two distinct robots r and r' in a configuration (G, λ) are *equivalent* if there exists $\varphi \in \text{Aut}(C)$ that makes equivalent the vertices in which they reside. Note that $\lambda(u) = \lambda(v)$ whenever u and v are equivalent. Moreover, if u and v are equivalent, a robot r cannot distinguish its position at vertex u from robot r' located at vertex $v = \varphi(u)$. As a consequence, no algorithm can distinguish between two equivalent robots.

In general, no algorithm can avoid that the two equivalent ASYNC robots start the computational cycle simultaneously. In such a case, there might be a so called *pending move* or *pending robot*, that is one of the two robots performs its entire computational cycle while the other has not started or not yet finished its Move phase. Formally, a robot r is pending in a configuration $C(t)$, if at time t robot r is active, has taken a snapshot $C(t') \neq C(t)$ with $t' < t$, and is planning to move or is moving with a non-nil trajectory. Clearly, any other robot r' is not aware whether there is a pending robot r , that is it cannot deduce such an information from the snapshot acquired in the Look phase. This fact greatly increases the difficulty to devise algorithms for symmetric configurations. Notice that all such difficulties are completely removed if an algorithm produces always *stationary* configurations: a configuration $C(t)$ is called *stationary* if there are no pending robots in $C(t)$. A way to produce stationary configurations is to guarantee that an algorithm always moves one robot at a time.

Concerning the configurations addressed in this work, it is not difficult to see that any $C = (G, \lambda)$, with $G \in \{G_S, G_T, G_H\}$, admits two types of automorphisms only: *reflections*, defined by a reflection axis which acts as a mirror; *rotations*, defined by a center and an angle of rotation. All the reflection axes are of two types: the reflection axes of the considered regular polygons and those coincident with any side of the regular polygons. The centers of possible rotations can be located only on specific

points of the regular polygons: on the center, on one vertex, or on the middle point of a side. The rotation angle is specific of each given tessellation graph.

2.3 The Arbitrary Pattern Formation (*APF*) problem

A configuration $C = (G, \lambda)$, with $G = (V, E)$, is *initial* if both the following conditions hold: (1) each robot is idle and placed on a different vertex, that is $\lambda(v) \leq 1$ for each $v \in V$; (2) C is asymmetric. The set containing all the initial configurations is denoted by \mathcal{I} .

The goal of the *APF* problem is to design a distributed algorithm \mathcal{A} that guides the robots to form a fixed arbitrary pattern F starting from any configuration $C = (G, \lambda)$ such that $G \in \{G_S, G_T, G_H\}$ and $C \in \mathcal{I}$. The pattern F is a multiset of vertices, given in any coordinate system, indicating the corresponding target vertices in the tessellation graph G . It constitutes the input for all robots. Due to absence of a common global coordinate system, the robots decide that the pattern is formed when the current configuration becomes “similar” to F with respect to translations, rotations, reflections. The problem can be formalized as follows: an algorithm \mathcal{A} solves the *APF* problem for an initial configuration C if, for each possible execution $\mathbb{E} : C = C(0), C(1), \dots$ of \mathcal{A} , there exists a finite time instant $t^* > 0$ such that $C(t^*)$ is similar to F and no robot moves after t^* , i.e., $C(t) = C(t^*)$ holds for all $t \geq t^*$.

2.4 Notation

Here we introduce some concepts and notation used to describe the proposed algorithm. Given a configuration $C = (G, \lambda)$, we use $R = \{r_1, r_2, \dots, r_n\}$ to denote the set containing all the n robots located on G (we recall that robots are anonymous and such a notation is used only for the sake of presentation). The distance $d(u, v)$ between two vertices $u, v \in V$ is the number of edges of a shortest path connecting u to v . We extend the notion of distance to robots: $d(r_i, r_j)$ denotes the distance between the two vertices in which the robots reside. Symbol $D(r)$ is used to denote the *sum of distances* of $r \in R$ from any other robot, that is $D(r) = \sum_{r_i \in R \setminus \{r\}} d(r, r_i)$.

Given a set of points P in the plane, $mbr(P)$ represents the *minimum bounding rectangle* of P , that is the rectangle enclosing all the points in P defined as follows: its sides are parallel to the Cartesian axes and each pair of parallel sides are as close as possible. According to the definition we get that $mbr(P)$ is unique. This definition can be easily extended to a set of robots R placed on the tessellation graph G_S where the canonical directions are just two, and they can naturally play the role of the Cartesian axes. Unfortunately, it does not work when R is placed on tessellation graphs such as G_T or G_H . To generalize it, we move to the concept of *bounding parallelogram* $bp(R)$, defined as any parallelogram enclosing all robots, with sides parallel to two of the three available canonical directions, and with each pair of parallel sides as close as possible. Since G_T or G_H admit three canonical directions, it can be observed that the bounding parallelogram of R is not unique. In fact, there are three possible bounding rectangles (e.g., see Fig. 3).

Given any $bp(R)$, we denote by $h(bp(R))$ and $w(bp(R))$, with $h(bp(R)) \leq w(bp(R))$, the width and height of $bp(R)$, respectively. Similarly, $h(bp(F))$ and $w(bp(F))$ are used to denote the same values with respect to $bp(F)$.

Let $bp(R)$ be any bounding parallelogram of R . We associate a sequence of integers to each canonical corner of $bp(R)$ (e.g., corners A and C in Fig. 3). The sequence associated with a canonical corner A is defined as follows. Scan the finite grid enclosed by $bp(R)$ from A along $h(bp(R))$ (say, from A to B) and sequentially all grid lines parallel to AB in the same direction. For each grid vertex

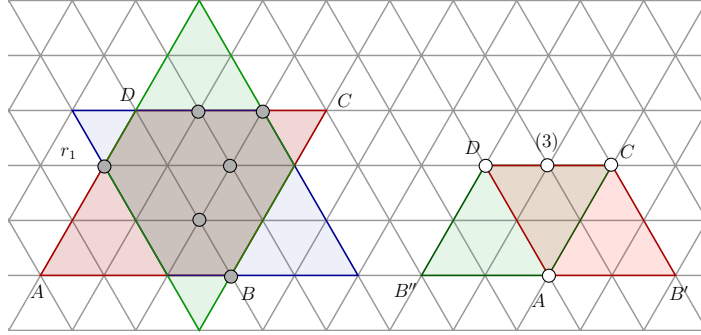


Fig. 3. (left) An initial configuration C with $n = 6$ robots. It shows that $bp(R)$ is not unique in G_T . The red parallelogram generates the LSS . The leading corner is A and the leading direction is AB . The unique LSS is $\ell = (0, 0, 0, 1, 0, 0, 1, 0, 1, 0, 1, 0, 0, 1, 1, 0)$. Notice that robot r_1 has maximum sum of distances, with value $D(r_1) = 13$. (right) A possible pattern F to be formed. The number close to a vertex refers to a multiplicity. Since F is symmetric, there are two (equivalent) $mbp(F)$.

v , put $\lambda(v)$ in the sequence. Denote the obtained sequence as $s(AB)$. Being $h(bp(R)) = w(bp(R))$ in the example, from A it is also possible to obtain the sequence $s(AD)$, and hence four sequences can be defined in total, two for the corner A and two for the corner C . If any two of these sequences are equal, then it implies that the configuration admits a (reflectional or rotational) symmetry. We denote by LSS the lexicographically smallest sequence. It is unique by definition.

The canonical corner from which an LSS starts is called the *leading corner*; the canonical direction from the leading corner used to create the LSS is called the *leading direction*. The LSS of a given $bp(R)$ is denoted as $\ell(bp(R))$, or simply as ℓ when $bp(R)$ can be inferred by the context.

Definition 2. Let $C = (G, \lambda)$ be a configuration with $G \in \{G_S, G_T, G_H\}$ and set of robot R . A minimum bounding parallelogram $mbp(R)$ is defined as any parallelogram $bp(R)$ with sides parallel to two canonical directions of G , with $h(bp(R))$ minimum, and with minimum LSS in case of ties.

Any asymmetric configurations admits exactly one $mbp(R)$ whereas symmetric configurations admit multiple $mbp(R)$'s. However, the LSS 's associated to such $mbp(R)$'s are all the same.

3 Description of the algorithm

In this section, we provide a high-level description of our algorithm \mathcal{A}_{form} designed to solve APF for any initial configuration $C = (G_T, \lambda)$ composed of n ASYNC robots endowed with the global strong multiplicity detection and with all the minimal capabilities recalled in Section 1.1. We assume $n \geq 3$, since for $n = 1$ the APF problem is trivial and for $n = 2$ we get that C is symmetric. Concerning the pattern F , it might contain multiplicities.

3.1 The strategy

In general, a single robot has rather weak capabilities with respect to the general problem it is asked to solve along with other robots (we recall that robots have no direct means of communication). For

this reason, any resolution algorithm should be based on a preliminary decomposition approach: the problem should be divided into a set of sub-problems so that each sub-problem is simple enough to be thought of as a “task” to be performed by (a subset of) robots. This subdivision could require several steps before obtaining the definition of such simple tasks, thus generating a sort of hierarchical structure.

Following this approach, *APF* is initially divided into four sub-problems denoted as Reference System (*RS*), Partial Pattern Formation (*PPF*), Finalization (*Fin*), and Termination (*Term*). Some of these sub-problems are further refined until the corresponding tasks can be suitably formalized according to the assumed capabilities of the robots. This leads to the following decomposition:

- *Reference System* ($RS = \text{How to embed } F \text{ on } G_T$). This sub-problem concerns one of the main difficulties arising when the general pattern formation problem is addressed: the lack of a unique embedding of F on G_T that allows each robot to uniquely identify its target (the final destination vertex to form the pattern). In particular, *RS* can be described as the problem of moving or matching some (minimal number of) robots into specific positions such that they can be used by any other robot as a common reference system. These robots are called *guards*. The realized reference system should imply a unique mapping from robots to targets, and this mapping should be maintained along all the movements of robots. In our strategy *RS* is further divided into three sub-problems denoted as RS_{1a} , RS_{1b} , and RS_2 . These sub-problems are simple enough to be associated to three tasks named T_1 , T_2 and T_3 , respectively. The first two are devoted to place the first guard denoted as r_1 , whereas the third fixes the position of a second guard denoted as r_n . Once such positions are reached by the two guards, the requested reference system is given by two lines passing through the vertices occupied by the guards and forming a canonical angle between them. When the reference system is created, all the robots except the guards result to be located in a specific quadrant called Q^- .
- *Partial Pattern Formation* ($PPF = \text{How to form part of } F$). This sub-problem is associated with task T_4 and it is addressed only once *RS* is solved. It concerns the formation of a pattern similar to part of F by using robots in $R'' = R \setminus \{r_1, r_n\}$ only. Thanks to the common reference system, all robots can agree on embedding F on a quadrant denoted as Q^+ and different from Q^- . During the task, all the $n - 2$ robots in R'' will be moved from Q^- to the quadrant Q^+ . Robots are moved one at a time so that no undesired collisions are created.
- *Finalization* ($Fin = \text{How to finally move } r_1 \text{ and } r_n \text{ so that } F \text{ is formed}$). It refers to the so-called finalization task and occurs when the only robots not well positioned according to F are the guards. It is worth to mention that while moving guards r_1 and r_n , the common reference system is lost. However, we are able to guarantee that robots can always detect they are solving *Fin* and that the two robots, by performing ad-hoc movements, can reach their targets so that the pattern F is correctly completed. *Fin* is divided into three tasks: T_5 concerns the movement of r_n , whereas T_6 and T_7 are related to the movement of r_1 .
- *Termination* (*Term*). It refers to the requirement of letting robots recognize the pattern has been formed, hence no more movements are required. In our strategy, a task T_8 is designed to address this problem. Clearly, only *nil* movements are allowed and it is not possible to switch to any other task.

In the remainder of the section we provide details for each designed task.

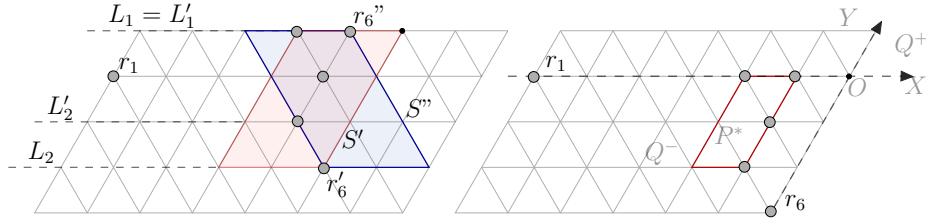


Fig. 4. (left) Visualization of sub-problem RS_{1a} concerning the initial movement of r_1 (cf. configuration C in Fig. 3). (right) Visualization of sub-problem RS_{1b} concerning the final destination of r_1 . Once r_1 stops, all the items necessary to define the reference system can be settled (cf Remark 1).

3.2 Task T_1

It selects a robot denoted as r_1 (the first guard) such that $D(r_1)$ is maximum (cf Fig. 3). In case of ties, r_1 has the minimum position in $\ell(\text{mbp}(R))$ – recall that the input configuration is asymmetric and hence $\text{mbp}(R)$ is unique. Let $R' = R \setminus \{r_1\}$, during this task r_1 moves through any shortest path toward to the closest vertex that satisfies the following Boolean variable:

- $\mathbf{g1} = \text{exists a unique line parallel to a canonical direction passing through } r_1 \text{ and each } bp(R')$.

Note that, when $\mathbf{g1}$ holds we identify the unique line passing through r_1 and each $bp(R')$ as the *line induced* by $\mathbf{g1}$.

3.3 Task T_2

In this task we assume true the variable $\mathbf{g1}$ holding at the end of task T_1 - this must be intended as a *pre-condition* imposed by our strategy in order to correctly perform T_2 . The main aim of this task is twofold: (1) to move r_1 so that its position allows to define the X -axis and (2) to identify the second guard r_n . Anyway, additional properties are guaranteed when the task is completed.

When the task starts, the role of r_1 is assigned to the robot r such that $D(r)$ is maximum whereas the second guard r_n is identified as follows:

- Let L be the line induced by $\mathbf{g1}$. It can be observed that there are exactly two distinct $bp(R')$'s with sides parallel to L . Let L_1 and L_2 be the two lines parallel to L shared by the two $bp(R')$'s (cf Fig. 4). Denote the two $bp(R')$'s as P' and P'' , and denote as S' (S'' , resp.) the side of P' (P'' , resp.) which lies neither on L_1 nor on L_2 and is further from r_1 . In particular, P' (P'' , resp.) is the parallelogram having the canonical angle formed by the intersection of S' (S'' , resp.) and L_1 (L_2 , resp.) - the red parallelogram in Fig. 4. Denote as r'_n (r''_n , resp.) the robot on S' (S'' , resp.) closest to L_1 (L_2 , resp.). The second guard useful to define the reference system is selected between r'_n and r''_n .

Robot r_1 considers the line L'_1 (L'_2 , resp.) defined as L_1 (L_2 , resp.) but referred to $R' \setminus \{r'_n\}$ ($R' \setminus \{r''_n\}$, resp.) instead of R' . Then r_1 selects the closest line between L'_1 and L'_2 (it arbitrarily selects one of the two in case of ties). Without loss of generality, assume that r_1 selects L'_1 . According to this choice, r_1 promotes r'_n to be r_n , that is the second guard (symmetrically, if r_1 selects L_2 , then r''_n is promoted).

After computing the second guard, the robots have enough information to identify the requested common reference system, as remarked in the following statement.

Remark 1. After computing the second guard, robots have sufficient information to compute a common reference system. In fact, the line between L'_1 and L'_2 selected by r_1 and letting all robots in R' in the same half-plane defines the X -axis, and this axis must be intended as directed from r_1 to all the other robots; all vertices in the half-plane containing robots in R' are considered with negative Y -coordinates. The second guard r_n is induced by the line between L'_1 and L'_2 selected by r_1 (as described above). The line passing through r_n , intersecting the X -axis, and forming a canonical angle in the first quadrant defines the Y -axis. Finally, the intersection between the two axes defines the origin of the system denoted as O . In this reference system, the first quadrant is denoted as Q^+ , while the third quadrant is denoted as Q^- .

Now, concerning the current task, it remains to be defined the correct positioning of both guards. The target of r_1 (r_n , resp.) is on the X -axis (Y -axis, resp.) so that the distance from the origin ensures that the configuration remains asymmetric during the subsequent *PPF* task. To define such a distance, robots compute the following:

- Let R^* be the (possibly empty) subset of robots of R'' lying in Q^- , P^* be the parallelogram $bp(R^*)$ with the constraint that it must use the directions parallel to the X - and Y -axes, and let $\Delta = \max\{w(P^*), w(mbP(F))\}$.⁴

According to Δ , the target of r_1 corresponds to the closest vertex on the X -axis which is at distance at least 3Δ from the origin. The trajectory followed is represented by any shortest path to the target. Note that at the end of task T_2 , variable $\mathbf{g1}$ still holds, but the movement of r_1 makes true the following additional variables:

- $\mathbf{hp}'' =$ all the robots in R'' are in the same half-plane with respect to the line induced by $\mathbf{g1}$.
- $\mathbf{dr1} = d(r_1, O) \geq 3\Delta$.

3.4 Task T_3

The aim of this task is to locate r_n to a destination easily recognizable in the next tasks, especially during the formation of the (sub-) pattern by robots in R'' . As a pre-condition, in this task we assume true all the variables holding at the end of task T_2 , namely $\mathbf{g1}$, \mathbf{hp}'' , and $\mathbf{dr1}$.

According to the pre-condition, in this task robots can use Remark 1, with the difference that now the X -axis is directly defined as the direction induced by $\mathbf{g1}$. By using that remark, robots can identify both guards and re-compute the common reference system. At this point, r_n performs the task by simply moving along the Y -axis (cf Fig. 5) toward the closest vertex $(0, y)$ such that the following variable holds:

- $\mathbf{gn} = r_n$ is at a vertex $(0, y)$, with $2\Delta \leq y < d(r_1, O)$.

The following additional remark states how robots can re-compute the common reference system in the subsequent tasks.

⁴ This definition of Δ is given with respect to R'' instead of R' so that it can be also used in the subsequent tasks T_3 , T_4 , and T_5 .

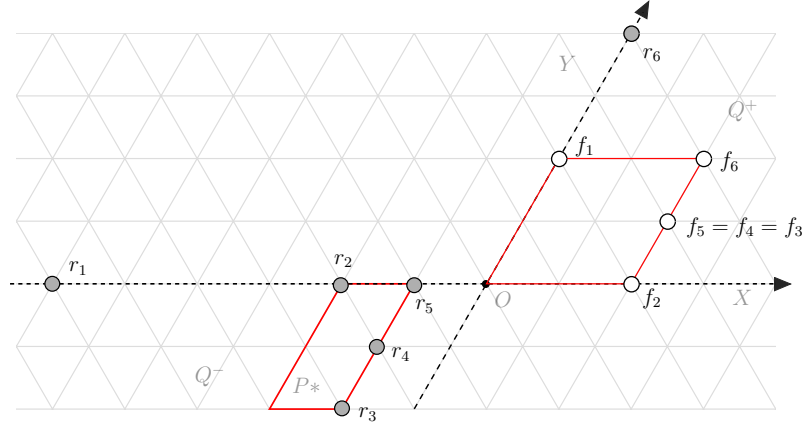


Fig. 5. Visualization of sub-problem RS_2 concerning the placing of guard $r_n = r_6$. Notice the embedding F_e in Q^+ (cf Definition 3) of the pattern represented in Fig. 3 and the ordering of all robots in R'' according to the lexicographic order of the coordinates of the vertices in which they reside.

Remark 2. At the end of Task T_3 , i.e. when both the guards are suitably placed, each robot can recognize the formed reference system: the two guards can be detected according to function $D()$, since r_1 and r_n have the largest and second largest value of $D()$, respectively; if $\mathbf{g1}$ holds, the induced line defines the X -axis directed from r_1 to all the other robots; the Y -axis is the line passing through r_n , intersecting the X -axis, directed from the intersection toward r_n , and forming a canonical angle in the first quadrant. Finally, the fact that the two guards are correctly positioned according to the strategy can be verified according to Δ , since Q^- (which contains all robots in R'') is identified.

3.5 Task T_4

This task concerns the so called “Partial Pattern Formation”, that is forming part of the input pattern F by using robots in $R'' = R \setminus \{r_1, r_n\}$ only. To this aim, all the $n - 2$ robots in R'' initially located in the quadrant Q^- will be moved in the quadrant Q^+ . In our strategy, it is addressed only once RS is solved, that is when the two guards r_1 and r_n are suitably placed. More formally, as a pre-condition for performing this task our algorithm requires that $\mathbf{g1}$, \mathbf{gn} , and $\mathbf{dr1}$ are all true.

It is clear that this task can be accomplished by robots in R'' only if they know the common reference system: this can be obtained as described in Remark 2. Concerning the partial pattern to be formed, all robots must agree on the positions they have to reach in Q^+ ; this problem is solved by performing an embedding of F into G_T according to the following definition.

Definition 3 (Embedding of the pattern). F_e is the set of vertices in Q^+ obtained by translating F so that the following conditions hold: (1) the leading corner of $\text{mbp}(F)$ is mapped onto the origin O , and (2) the leading direction of $\text{mbp}(F)$ coincides with the positive direction of the Y -axis.

An example of F_e is shown in Fig. 5. Once the robots agree on F_e , the main difficulties in this task are to preserve the reference system (induced by guards r_1 and r_n) and to avoid undesired collisions during the movements. To avoid collisions, robots are moved one at a time according to a schedule induced by the following definitions:

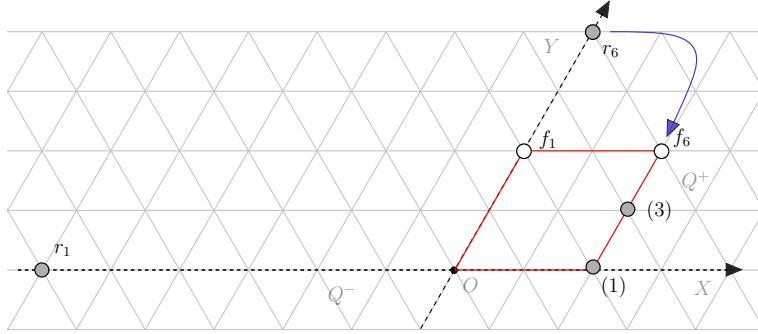


Fig. 6. Visualization of the configuration obtained at the end of task T_4 (cf Fig.5). Gray (black, white, resp.) circles represent unmatched robots (matched robots, unmatched targets, resp.), while integers close to matched robots refer to multiplicities.

- Vertices in F_e are ordered according to the lexicographic order of their coordinates expressed according to the formed X - and Y -axes. Hence, from now on we denote F_e as the multiset⁵ $\{f_1, f_2, \dots, f_n\}$, where $i \leq j$ if and only if the coordinates of f_i precede those of f_j . Similarly for robots in R'' : they are ordered according to the lexicographic order of the coordinates of the vertices in which they reside and $R'' = \{r_2, r_3, \dots, r_{n-1}\}$.
- Vertices f_1 and f_n are not used during the resolution of PPF since they are considered as the final *targets* for the guards. In particular, in the last part of the resolution algorithm, r_1 will be moved in f_1 and r_n will be moved in f_n .
- A vertex $f_i \in F_e$, $2 \leq i \leq n-1$, is called the *largest unmatched target* if it is unoccupied whereas f_j is occupied for each $i < j < n$.
- A robot $r_i \in R''$, $2 \leq i \leq n-1$, is called *largest unmatched robot* if f_i is the largest unmatched target.

Algorithm \mathcal{A}_{form} moves robots in R'' in order, moving each time the largest unmatched one toward the largest unmatched target in F_e . The trajectory of a moving robot is given by any shortest path leading to its target.

During the task, all the unmatched robots must result to be correctly positioned with this strategy. This is controlled by the following variable:

- **rpf** = the largest unmatched robot r_i is on a shortest path from any vertex in Q^- to f_i , and each robot r_j , $j < i$, is in Q^- .

Notice that at the end of this task, variable **g1** still holds. Finally, also the following additional variables hold:

- **hp'** = all the robots in R' are in the same half-plane with respect to the line induced by **g1**.
- **pfn** = there exists an embedding of F such that all robots in R'' are similar to $F \setminus \{f_1, f_n\}$

⁵ Recall that F may contain multiplicities.

3.6 Task T_5

This task is the first associated with “Finalization” sub-problem. In particular, it concerns the movement of r_n toward f_n . According to the strategy, our algorithm assumes that all the variables made true by the previous task T_4 are true, namely $\mathbf{g1}$, \mathbf{hp}' , $\mathbf{dr1}$, and \mathbf{pfn} .

Robot r_n moves from the Y -axis straightly along the canonical direction parallel to the X -axis until a vertex with the same X -coordinate of f_n is reached, and then it directly proceeds toward the target (cf. Fig. 6). The movement of r_n can take many LCM cycles and hence it is required a new variable to check the correct positioning of r_n :

- $\mathbf{hrn} = \text{point } f_n = (x, y) \text{ and robot } r_n = (x', y'), \text{ with } x' \leq x \text{ and } y' \geq y.$

Clearly, the check of variable \mathbf{hrn} requires the reference system. However, this cannot be evaluated as it has been done in the previous tasks, since r_n is currently moving (i.e., guards are not suitably placed anymore). Anyway, since \mathbf{pfn} holds, the reference system can be deduced from the embedding. In particular:

Remark 3. During Task T_5 , each robot can recognize the formed reference system: r_1 can be detected according to function $D()$ since it has the largest value of $D()$; if $\mathbf{g1}$ and \mathbf{hp}' hold, the induced line defines the X -axis directed from r_1 to all the other robots; from $\text{mbp}(F)$ it is possible to check whether its leading corner placed on a vertex v on the X -axis makes f_2, \dots, f_{n-1} matched, hence defining r_n ; the Y -axis is assumed as the canonical direction passing through v and forming a canonical angle in the first quadrant which contains all robots in R' ; finally, knowing r_1 and r_n and Q^- it is possible to compute Δ and hence check whether $\mathbf{dr1}$ holds.

Once r_n reaches f_n , variables $\mathbf{g1}$, $\mathbf{dr1}$ still hold and a new variable is made true:

- $\mathbf{pf1} = \text{pattern } F \setminus \{f_1\} \text{ formed.}$

3.7 Tasks T_6 and T_7

When T_6 starts as a consequence of the termination of T_5 , variables $\mathbf{g1}$, $\mathbf{dr1}$, and $\mathbf{pf1}$ are all true. This means that $n - 1$ robots reached their targets apart from one robot which is far enough from the others in order to induce just one direction toward the remaining robots. From now on such a robot is referred to as r_1 . Since T_6 and T_7 refer to the “Finalization” sub-problem, r_1 must be moved toward its target in order to finalize the pattern F . This means that during such tasks both guards are no longer correctly positioned and hence the common reference system is no longer available. In particular, the origin O of the system is not defined and hence $\mathbf{dr1}$ cannot be evaluated. Anyway, we will see that the algorithm will move r_1 so that the following variable remains valid during T_6 :

- $\mathbf{dr1}' = \text{the distance between } r_1 \text{ and the other robots guarantees that } d(r_1, \text{mbp}(F)) \geq 3w(\text{mbp}(F)).$

In particular, task T_6 is meant to move r_1 toward a target vertex t so that the following properties hold: (1) $\mathbf{dr1}'$ remains true, and (2) in the subsequent task T_7 , starting from t , robot r_1 can reach its final destination f_1 by moving straightly along one canonical direction.

Even if in both T_6 and T_7 the common reference system is no longer available, robots can take advantage of the existing positions of r_1 and of the other robots to correctly finalize the pattern. In particular, when T_6 starts the variables $\mathbf{g1}$, $\mathbf{dr1}'$, and $\mathbf{pf1}$ are all true and, accordingly, robots can compute the following data:

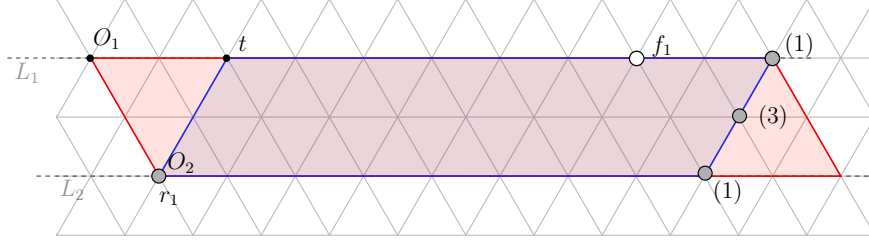


Fig. 7. Visualization of the configuration obtained at the end of task T_5 (cf Fig.6). Gray (black, white, resp.) circles represent unmatched robots (matched robots, unmatched targets, resp.), while integers close to matched robots refer to multiplicities.

- let U be the direction induced by variable $\mathbf{g1}$. Let L_1 and L_2 be the lines parallel to U , closest to each other, and enclosing $R' = R \setminus \{r_1\}$;
- consider the smallest parallelogram P_1 (P_2 , resp.) such that: it encloses the whole set R , it guarantees $h(P_1) = h(mbP(F))$, it has the longest side on L_1 (L_2 , resp.), and it determines a corner O_1 (O_2 , resp.) at the intersection vertex with the shortest side passing through r_1 that admits a canonical angle;
- compute sP_1 (sP_2 , resp.) as the sequence of integers associated with O_1 (O_2 resp.) such that r_1 is met as the first robot.

As an example, P_1 and P_2 correspond to the red and blue parallelograms represented in Fig. 7, respectively. According to such data, robots can verify whether the current configuration is coherent with task T_6 of our algorithm \mathcal{A}_{form} by performing the following check:

- at least one parallelogram between P_1 and P_2 must be coherent with the $n - 1$ elements of F already matched. This means that the last values of sP_1 (or sP_2) must coincide with the sequence $\ell(mbP(F))$ except for just one value corresponding to f_1 (the vertex to be matched by r_1). Notice that it is possible that this happens for both sP_1 and sP_2 when there is a reflection axis for $F \setminus \{f_1\}$ parallel to the direction U .

If we denote by $\ell_{f_1}^F$ the sequence of integers obtained from $\ell(mbP(F))$ by decreasing by one the first non-zero element,⁶ and by d_f the position in $\ell(mbP(F))$ of such an element, the above check can be done by better formalizing variable $\mathbf{pf1}$:

- $\mathbf{pf1} =$ there exists $s \in \{sP_1, sP_2\}$ such that $s = s' + \ell_{f_1}^F$, for some s' made of only 0's and just one 1 in position d_{r_1} and $d_{r_1} < d_f$.

Referring to the example shown in Fig. 7, variable $\mathbf{pf1}$ is made true by the sequence obtained from the vertex O_2 . In fact, $sP_2 = (1, 0, 0, 0^{21}, 1, 3, 1)$, $\ell(mbP(F)) = (0, 0, 1, 0, 0, 0, 1, 3, 1)$, $d_{r_1} = 1$ and $d_f = 3$.

During T_6 , robot r_1 is moved along the shortest side of the parallelogram associated with the string s (cf. the definition of $\mathbf{pf1}$) so as to increase position d_{r_1} . This movement stops when $d_{r_1} = d_f$ applies and at that time task T_7 starts. It is easy to observe that when T_7 starts as a consequence of the termination of T_6 , the following variable holds:

⁶ Basically $\ell_{f_1}^F$ denotes the sequence $\ell(mbP(F))$ by ignoring f_1 .

- **qf1** = sequence $\ell(\text{mbp}(R))$ guarantees that $\ell(\text{mbp}(R)) = \ell' + \ell_{f_1}^F$, for some ℓ' made of only 0's and just one 1 in position d_{r_1} and $d_{r_1} = d_f$.

Basically, when **qf1** holds, all robots know that r_1 can complete the pattern by going straight toward its target. The main difficulty in this task is to cope with possible symmetries formed during the last movement of r_1 . Notice that the configurations produced by the algorithm are always asymmetric (this holds for the initial configuration, and the position of r_1 guarantees that this property is maintained in T_1, \dots, T_6). In principle, when r_1 is very close to its target, possible symmetries may imply that more than one robot can detect itself as the moving robot r_1 , and also that r_1 can detect more than one vertex as the target f_1 . However, we are able to show that in any case the formed configuration has at most a reflection axis with r_1 on that axis. Summarizing, we will show that all these cases do not prevent the algorithm to complete the pattern formation.

4 Formalization and correctness

As introduced in the previous section, the proposed algorithm \mathcal{A}_{form} is based on a strategy that decomposes the *APF* problem into tasks T_1, T_2, \dots, T_8 . According to the LCM model, during the **Compute** phase each robot must be able to recognize the task to be performed just according to the configuration perceived during the **Look** phase and the input pattern F . This recognition can be performed by providing \mathcal{A}_{form} with a *predicate* P_i for each task T_i . Given the perceived configuration and the input pattern F , the predicate P_i that results to be true reveals to robots that the corresponding task T_i is the task to be performed. This approach requires that the designed predicates must guarantee some properties:

- Prop₁**: given the pattern F , each P_i must be computable on the configuration C perceived in each **Look** phase;
- Prop₂**: $P_i \wedge P_j = \text{false}$, for each $i \neq j$; this property allows robots to exactly recognize the task to be performed;
- Prop₃**: given the pattern F , for each possible perceived configuration C there must exist a predicate P_i evaluated true.

If we guarantee that all these properties hold, then \mathcal{A}_{form} can be used in the **Compute** phase as follows:

- if a robot r executing algorithm \mathcal{A}_{form} detects that predicate P_i holds, then r simply performs a move m_i associated with task P_i .

Concerning how to define the predicates, we have already remarked in the previous section that each task can be accomplished only when some *pre-conditions* are fulfilled. Hence, to define the predicates in general we need:

- *basic variables* that capture metric/topological/numerical/ordinal aspects of the input configuration which are relevant for the used strategy and that can be evaluated by each robot on the basis of its view;
- *composed variables* that express the pre-conditions of each task T_i .

All the needed basic variables useful for \mathcal{A}_{form} have been already defined in Sections 3.2–3.7. If we assume that pre_i is the composed variable that represents the pre-conditions of P_i , for each $1 \leq i \leq 8$, then predicate P_i can be defined as follow:

$$P_i = \text{pre}_i \wedge \neg(\text{pre}_{i+1} \vee \text{pre}_{i+2} \vee \dots \vee \text{pre}_8) \quad (1)$$

This definition leads to the following remark:

<i>var</i>	<i>definition</i>	<i>rationale</i>
g1	\exists a unique line parallel to a canonical direction passing through r_1 and each $bp(R')$	<i>guard r_1 is partially placed</i>
gn	r_n is at a vertex $(0, y)$, with $2\Delta \leq y < d(r_1, O)$	<i>guard r_n is placed</i>
dr1	$d(r_1, O) \geq 3\Delta$	<i>guard r_1 is at a desired distance from the origin</i>
dr1'	$d(r_1, mbp(F)) \geq 3w(mbp(F))$	<i>robot r_1 is at a desired distance from the pattern</i>
hp'	let L be the line induced by g1 ; all robots in R' are in the same half-plane with respect to L	<i>all robots in R' are in the same half-plane with respect to the line induced by g1</i>
hp''	let L be the line induced by g1 ; all robots in R'' are in the same half-plane with respect to L	<i>all robots in R'' are in the same half-plane with respect to the line induced by g1</i>
hrn	$f_n = (x, y)$ and $r_n = (x', y')$, with $x' \leq x$ and $y' \geq y$	<i>guard r_n is on the right path to its target</i>
rpf	the largest unmatched robot r_i is on a shortest path from any vertex in Q^- to f_i , and each robot r_j , $j < i$, is in Q^-	<i>all the unmatched robots are correctly positioned with respect to PPF</i>
pf1	$\exists s \in \{sP_1, sP_2\}$: $s = s' + \ell_{f_i}^F$, for some s' made of only 0's and just one 1 in position d_{r_1} and $d_{r_1} < d_f$	<i>pattern $F \setminus \{f_1\}$ formed</i>
pfn	\exists embedding of F such that all robots in R'' are similar to $F \setminus \{f_1, f_n\}$	<i>pattern $F \setminus \{f_1, f_n\}$ formed</i>
qf1	$\ell(mbp(R)) = \ell' + \ell_{f_i}^F$, for some ℓ' made of only 0's and just one 1 in position d_{r_1} and $d_{r_1} = d_f$	<i>guard r_1 can complete the pattern by going straight toward its target</i>
s	R and F are similar	<i>pattern F formed</i>

Table 1. The basic Boolean variables used to define all the tasks' preconditions.

Remark 4. Predicates P_i fulfill Property **Prop**₂. This is directly implied by Eq. 1

Before addressing the remaining properties **Prop**₁ and **Prop**₃, we formalize all the basic variables, the pre-conditions for each task, and, as a consequence, all the predicates. All the necessary basic variables are summarized in Table 1. Table 2 reports all the ingredients determined by the proposed algorithm: the first two (general) columns recall the hierarchical decomposition described in the previous section, the third column associates tasks names to sub-problems, and the fourth column defines precondition **pre** _{i} for each task T_i . These preconditions must be considered according to Equation 1. The fifth column of Table 2 contains the name of the move used in each task (we simply denote as m_i the move used in task T_i), and the specification of each move is provided in Table 3. Unless differently specified, each trajectory defined in the moves must be intended as any shortest path to the target.

Table 2 leads to the following remark:

<i>problem</i>	<i>sub-problem</i>	<i>task</i>	<i>precondition</i>	<i>move</i>	
<i>APF</i>	<i>RS</i>	<i>RS</i> _{1a}	<i>T</i> ₁	<i>true</i>	<i>m</i> ₁
		<i>RS</i> _{1b}	<i>T</i> ₂	<i>g1</i>	<i>m</i> ₂
		<i>RS</i> ₂	<i>T</i> ₃	<i>g1</i> \wedge <i>hp''</i> \wedge <i>dr1</i>	<i>m</i> ₃
	<i>PPF</i>		<i>T</i> ₄	<i>g1</i> \wedge <i>dr1</i> \wedge <i>gn</i> \wedge <i>rpf</i>	<i>m</i> ₄
	<i>Fin</i>	<i>Fin</i> ₁	<i>T</i> ₅	<i>g1</i> \wedge <i>hp'</i> \wedge <i>dr1</i> \wedge <i>hrn</i> \wedge <i>pfn</i>	<i>m</i> ₅
		<i>Fin</i> ₂	<i>T</i> ₆	<i>g1</i> \wedge <i>dr1'</i> \wedge <i>pf1</i>	<i>m</i> ₆
		<i>Fin</i> ₃	<i>T</i> ₇	<i>qf1</i>	<i>m</i> ₇
	<i>Term</i>		<i>T</i> ₈	<i>s</i>	<i>nil</i>

Table 2. Algorithm \mathcal{A}_{form} for *APF*.

<i>move</i>	<i>definition</i>
<i>m</i> ₁	<i>r</i> ₁ moves toward the closest vertex so as <i>g1</i> holds
<i>m</i> ₂	<i>r</i> ₁ moves on the closest vertex on <i>X</i> -axis at distance at least 3Δ from the origin
<i>m</i> ₃	<i>r</i> _{<i>n</i>} moves toward vertex $(0, y)$, with $2\Delta \leq y < d(r_1, O)$
<i>m</i> ₄	the <i>largest unmatched robot</i> in R'' moves toward the <i>largest unmatched target</i> in F_e
<i>m</i> ₅	<i>r</i> _{<i>n</i>} first moves along a path that maintains fixed the <i>y</i> coordinate until its <i>x</i> coordinate coincides with that of <i>f</i> _{<i>n</i>} - then, it moves toward <i>f</i> _{<i>n</i>}
<i>m</i> ₆	if both <i>sP</i> ₁ and <i>sP</i> ₂ satisfy <i>pf1</i> then let <i>s</i> be the lexicographically minimum one. Then, robot <i>r</i> ₁ moves along the shortest side of the parallelogram associated with <i>s</i> so as to increase d_{r_1}
<i>m</i> ₇	robot <i>r</i> ₁ in position d_{r_1} moves toward <i>f</i> ₁

Table 3. Moves associated with tasks. It is assumed that each robot not involved in m_i perform the *nil* movement.

Remark 5. Algorithm \mathcal{A}_{form} fulfills Property **Prop**₃. This is implied by pre-condition **pre**₁ and predicates P_i .

4.1 On computing the predicates: property **Prop**₁

In this section, we show how the proposed algorithm \mathcal{A}_{form} can compute each predicate P_i , that is, we show that \mathcal{A}_{form} guarantees that property **Prop**₁ holds.

According to the definition of P_i given in Eq. 1, in the **Compute** phase, each robot evaluates – with respect to the perceived configuration C and the pattern F to be formed – the predicates starting from P_8 and proceeding in the reverse order with the others until a true pre-condition is found. In case all pre-conditions **pre**₈, **pre**₇, ..., **pre**₂ are evaluated false, then task P_1 is performed.

Evaluating **pre**₈ is just a matter of testing whether C and F are similar. Concerning the evaluation of **pre**₇, robots need to compute just variable **qf1**, which in turn depends only on $mbp(R)$ and $mbp(F)$.

Pre-condition pre_6 implies to compute $\mathbf{g1}$, $\mathbf{dr1}'$, and $\mathbf{pf1}$: the first needs r_1 , which can be identified according to function $D()$ since in all tasks T_1, \dots, T_6 this guard corresponds to the robot r such that $D(r)$ is maximum; the second just uses r_1 and $\text{mbp}(F)$; the third is computable as shown in Section 3.7 starting from the direction U induced by variable $\mathbf{g1}$, and by using U and $\text{mbp}(F)$ to determine the sequences sP_1 and sP_2 , and the positions d_{r_1} and d_f .

Pre-condition $\text{pre}_5 = \mathbf{g1} \wedge \mathbf{hp}' \wedge \mathbf{dr1} \wedge \mathbf{hrn} \wedge \mathbf{pfn}$ can be evaluated as follows: $\mathbf{g1}$ can be evaluated once r_1 has been recognized thanks to function $D()$, and \mathbf{hp}' can be detected once the direction induced by variable $\mathbf{g1}$ is known. Now, as described in Remark 3, by using $\mathbf{g1}$ and \mathbf{hp}' the common reference system can be established by each robot, and from it both $\mathbf{dr1}$ and \mathbf{hrn} can be evaluated. Finally, variable \mathbf{pfn} can be checked by using a combinatorial approach.

Concerning pre-condition $\text{pre}_4 = \mathbf{g1} \wedge \mathbf{dr1} \wedge \mathbf{gn} \wedge \mathbf{rpf}$, all its variables except \mathbf{rpf} can be evaluated according to Remark 2, while \mathbf{rpf} can be easily checked according to the definitions introduced in Section 3.5. Pre-condition $\text{pre}_3 = \mathbf{g1} \wedge \mathbf{hp}'' \wedge \mathbf{dr1}$ can be evaluated as follows: $\mathbf{g1}$ can be computed again according to $D()$, and then Remark 1 can be used to establish the common reference system. From this reference system, both \mathbf{hp}'' and $\mathbf{dr1}$ can be evaluated.

Finally, for checking $\text{pre}_2 = \mathbf{g1}$ it is enough to use $D()$ to identify robot r_1 .

4.2 Correctness

In this section, we formally prove that algorithm \mathcal{A}_{form} solves the APF problem on the tessellation graph G_T . To this end, let \mathcal{I}_A be the set containing all the configurations taken as input or generated by \mathcal{A}_{form} .

According to properties Prop2 and Prop3, all tasks' predicates P_1, P_2, \dots, P_8 used by the algorithm have been defined so as to make a partition of \mathcal{I}_A . Together with Prop1, for each possible configuration provided to \mathcal{A}_{form} , the algorithm can evaluate each predicate and exactly determine the task to be performed.

The correctness can be assessed by proving that all the following properties hold:

- H_1 : \mathcal{A}_{form} does not generate multiplicities nor symmetric configurations (unless F is formed or its formation is not prevented);
- H_2 : from any class T_i , $1 \leq i \leq 8$, no class T_j with $j < i$ can be reached.
- H_3 : from any class T_i , $1 \leq i \leq 7$, another class T_j with $j > i$ is always reached within a finite number of LCM cycles.

Since properties H_1 , H_2 and H_3 must be proved for each transition/move, then in the following we provide a specific lemma for each task.

Lemma 1. *From an initial configuration C belonging to class $T_1 \cap \mathcal{I}_A$ the algorithm \mathcal{A}_{form} eventually leads to a configuration C' in a class T_i , $i > 1$.*

Proof. In this task, algorithm \mathcal{A}_{form} selects a robot denoted as r_1 (the first guard) such that $D(r_1)$ is maximum and, in case of ties, the robot that has the minimum position in $\ell(\text{mbp}(R))$.

H_1 . Since $D(r_1)$ is maximum, while r_1 moves away from the other robots, it cannot meet any other robot and $D(r_1)$ increases. Then, r_1 is repeatedly selected. Note that, if by m_1 a symmetric configuration is created then it must admit an axis of reflection where r_1 lies as this is the only robot defining $D(r_1)$.

H_2 . Since as we are going to show the subsequent H_3 holds, we have that any other class can be reached.

H_3 . Robot r_1 always decreases the distance toward its target, within a finite number of LCM cycles, unless other predicates become true, $\mathbf{g1}$ becomes true and the configuration is not in T_1 anymore. \square

Lemma 2. *From a configuration C belonging to class $T_2 \cap \mathcal{I}_A$ the algorithm \mathcal{A}_{form} eventually leads to a configuration C' in a class T_i , $i > 2$.*

Proof. Here r_1 lies between two parallel directions L_1 and L_2 enclosing each possible $bp(R')$ and moves toward the closest one (toward any of them in case of ties) along a canonical direction.

H_1 . Robot r_1 , when moving toward its target, cannot meet any other robot, nor move on any axis of symmetry because the only possible one should be at the same distance from L_1 and L_2 and parallel to them. However, by moving to the closest L_i , $i \in \{1, 2\}$, r_1 never crosses an axis.

H_2 . Move m_2 does not affect predicate $\mathbf{g1}$, that is no obtained configuration can belong to T_1 .

H_3 . Robot r_1 always decreases the distance toward L_i , then within a finite number of LCM cycles, unless other predicates become true, $\mathbf{hp}'' \wedge \mathbf{dr1}$ becomes true (cf. Section 3.3) and the configuration is not in T_2 anymore. \square

Lemma 3. *From a configuration C belonging to class $T_3 \cap \mathcal{I}_A$ the algorithm \mathcal{A}_{form} eventually leads to an asymmetric configuration C' in T_i , $i > 3$.*

Proof. During this task, guard r_1 is already placed, that is $\mathbf{g1} \wedge \mathbf{hp}'' \wedge \mathbf{dr1}$ holds.

H_1 . Due to the positioning of r_1 , the configuration can be symmetric only when all robots are collinear (along the formed X -axis). Regardless when this symmetry is formed, during this task, r_n is always detected and as soon as it leaves the X -axis, the configuration becomes asymmetric and remains as such until the second guard terminates its trajectory. According to m_3 , along its movement r_n cannot meet any other robot. Notice that, according to the different distances of the two guards from O , the configuration cannot admit rotations nor reflections as long as the guards are idle.

H_2 . Move m_3 does not affect predicates $\mathbf{g1}$, \mathbf{hp}'' and $\mathbf{dr1}$, that is any obtained configuration cannot belong to T_1 nor to T_2 .

H_3 . Robot r_n always decreases the distance toward its target along the Y -axis, then within a finite number of LCM cycles, unless other predicates become true, \mathbf{gn} becomes true. In any case the configuration is not in T_3 anymore. \square

Lemma 4. *From any configuration C belonging to class $T_4 \cap \mathcal{I}_A$ the algorithm \mathcal{A}_{form} eventually leads to a configuration C' in T_5 .*

Proof. H_1 . Since guards r_1 and r_n are placed, the same considerations of Lemma 3 hold, that is the configuration cannot admit reflections nor rotations during this task. Multiplicities can be created but only if required by the formation of F .

H_2 . During the whole task, predicate \mathbf{s} is false as guards remain placed. Hence, also predicates $\mathbf{g1}$, $\mathbf{dr1}$, \mathbf{gn} and \mathbf{rpf} are not affected by m_4 , that is the obtained configuration cannot belong to T_1 , T_2 , and T_3 .

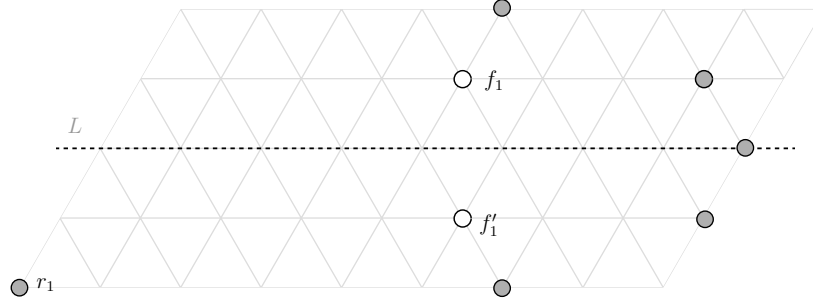


Fig. 8. An example of the only possible symmetry that can arise during task T_6 .

H_3 . While the task is performed, either the number of matched robots increases or the distance of one robot from its target decreases, then in a finite number of moves all robots excluding r_1 and r_n will be matched. As already described in Section 3.5, at the end of this task $\mathbf{g1} \wedge \mathbf{hp}' \wedge \mathbf{dr1} \wedge \mathbf{hrn} \wedge \mathbf{pfn}$ holds, that is C' belongs to T_5 and no other task can be reached because the guards remain placed. \square

Lemma 5. *From any configuration C belonging to class $T_5 \cap \mathcal{I}_A$ the algorithm \mathcal{A}_{form} eventually leads to a configuration C' in T_i , $i > 5$.*

Proof. During this task, guard r_1 remains placed.

H_1 . As r_n moves toward its final target, the arisen configurations cannot admit reflections nor rotations as there are no other robots equivalent to r_1 due to $\mathbf{g1}$ and $\mathbf{dr1}$. A reflection (as well as a multiplicity, resp.) can occur only at the end of the task if all robots are collinear (if f_n requires a multiplicity, resp.) but this can be managed by \mathcal{A}_{form} as we are going to see in the next lemma devoted to T_6 .

H_2 . Before r_n reaches its target, $\mathbf{g1} \wedge \mathbf{hp}' \wedge \mathbf{dr1} \wedge \mathbf{hrn} \wedge \mathbf{pfn}$ remains true, while predicates $\mathbf{pf1}$ and \mathbf{s} remain false, that is the configuration remains in T_5 . Once r_n reaches f_n , predicate $\mathbf{g1} \wedge \mathbf{dr1}' \wedge \mathbf{pf1}$ becomes true.

H_3 . After each move, r_n decreases its distance from f_n , that is within a finite number of LCM cycles the task ends and, unless other predicates become true, the obtained configuration C' belongs to T_6 . \square

Lemma 6. *From a configuration C belonging to class $T_6 \cap \mathcal{I}_A$ the algorithm \mathcal{A}_{form} eventually leads to a configuration C' in T_7 .*

Proof. During this task, guard r_1 moves so as to make $d_{r_1} = d_{f_1}$.

H_1 . During this phase the algorithm does not generate any multiplicity since $\mathbf{g1} \wedge \mathbf{dr1}' \wedge \mathbf{pf1}$ remains true and then r_1 is sufficiently far from any other robot. Regarding symmetries (cf. Figure 8), the only symmetric configuration possible is the one with an axis parallel to the direction induced by $\mathbf{g1}$, and f_1 can be on the axis or not. In the first case, the whole pattern is symmetric; when r_1 reaches the axis then $d_{r_1} = d_{f_1}$ holds and predicate $\mathbf{qf1}$ becomes true. Otherwise the final pattern is asymmetric and there are two possible embeddings and two possible targets for r_1 , f_1

and its equivalent point f'_1 with respect to the axis of symmetry. One of the two is reachable by r_1 without crossing the axis. Targets f_1 and f'_1 lie in the same half plane or not. In the first case only one among the sequences sP_1 and sP_2 satisfies the condition in **pf1** because in one of them $d_{r_1} > d_{f_1}$. Then r_1 moves towards f_1 and when it reaches the height of f'_1 predicate **qf1** becomes true and the configuration is in T_7 . When r_1 lies between f_1 and f'_1 , both the sequences sP_1 and sP_2 satisfy the condition in **pf1** and move m_6 chooses the smaller one since sP_1 and sP_2 must be different because r_1 is not on the axis. Robot r_1 increases its height to align with the target until $d_{r_1} = d_{f_1}$ and the configuration is in T_7 .

H_2 . Before r_1 reaches the height of its target, $\mathbf{g1} \wedge \mathbf{dr1}' \wedge \mathbf{pf1}$ remains true, and when $d_{r_1} = d_{f_1}$, **qf1** holds, hence C' is in T_7 . Clearly C' cannot belong to T_8 .

H_3 . The absolute difference between d_r and d_f decreases by one at each move until $d_{r_1} = d_{f_1}$ so that move m_6 is applied only a finite number of times. \square

Lemma 7. *From a configuration C belonging to class $T_7 \cap \mathcal{I}_A$ the algorithm \mathcal{A}_{form} eventually leads to a configuration C' in T_8 .*

Proof. During this task, guard r_1 straightly moves toward its target. Since **qf1** holds it is possible to derive the embedding of the pattern from $\ell(mbp(F))$ and consequently the X and Y axis that we refer to the proof.

H_1 . We show that while r_1 moves toward f_1 no reflections, no rotations, no multiplicities can be created that prevent the finalization of the task. In particular, we first show that no rotations are possible, then we analyze reflections showing that none of them can admit a robot equivalent to r_1 . Hence, if a reflection is created, then r_1 must be on the axis of symmetry, and we show this happens only if $F \setminus \{f_1\}$ is symmetric respect to that axis. Regarding the multiplicities, r_1 can make one only once f_1 is reached.

Rotations. The minimal possible angle of rotation is 60° and its multiples 120° and 180° , clockwise and anti-clockwise. The convex hull of any configuration with rotational symmetry with angle of rotation of 60° is an hexagon. Assuming that such a configuration is formed when r_1 is approaching its target, a part of the convex hull should be in the quadrant where r_1 lies. Then the embedding of the pattern is not positioned according to the rule that the shorter side of the parallelogram is parallel to the Y -axis (cf Definition 3). With the same arguments we can exclude rotations of 120° . Regarding to rotations of 180° , let us assume that r_1 creates such a symmetry when approaching its target. The embedding F_e is done by construction in such a way that the sequence of integers read from the origin is smaller than the one read from the corner $P = (x_p, y_p)$ at the opposite angle of 60° . The first column read from P must have a single robot r'_1 , symmetric to r_1 , because this column matches the one with r_1 .

By hypothesis, the pattern sequence read from O must be lower than the one read from P , then the first column cannot have more than one target and in particular this target must be at the same distance from O than r'_1 from P , because r_1 is moving horizontally. Reading the configuration forward from P , there must be a sequence of columns of zeros, at least one, each corresponding to an empty column read from r_1 to the Y -axis, that is empty. In turn, this corresponds to a sequence of columns of zeros in the pattern read from O , because by hypothesis must be lower than the one read from P . Then, by rotation, these columns correspond to more empty columns in the configuration read from P . Continuing, we would have only empty columns between r_1 and r'_1 , contradicting the hypothesis that the robots are at least three.

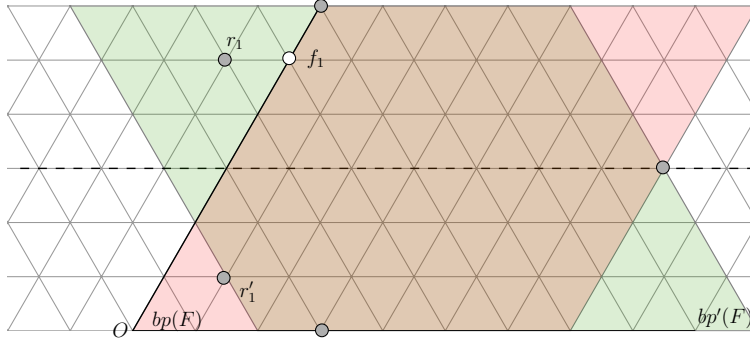


Fig. 9. An example in which r_1 becomes equivalent to another robot r'_1 respect to an axis of 0° while moving toward f_1 .

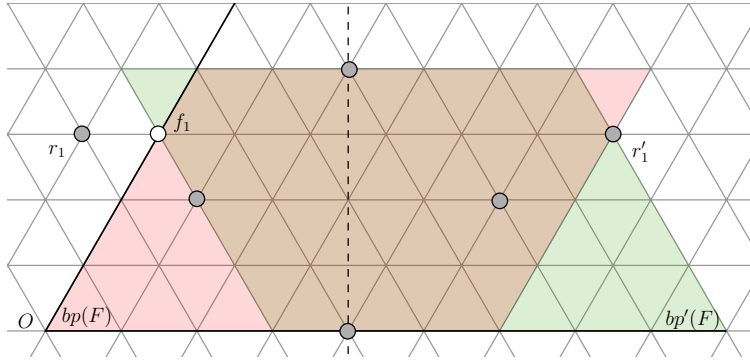


Fig. 10. An example in which r_1 becomes equivalent to another robot r'_1 respect to an axis of 90° while moving toward f_1 .

Reflections. Regarding reflections we have to analyze possible axis of reflection at 0° , 30° , 60° , 90° , 120° , 150° , with respect to the X -axis in clockwise direction. Moreover we distinguish between two cases: when r_1 becomes equivalent to another robot of the configuration and when r_1 goes on an axis of symmetry.

Firstly, we analyze the case of a reflection at 0° when r_1 becomes equivalent to another robot r'_1 while moving toward f_1 . Now consider the other possible $bp'(F)$ having two sides parallel to the X -axis and shared with the chosen $bp(F)$. One side of $bp'(F)$ passes through r'_1 and the reading from this side is lower than the reading of $bp(F)$ from the origin. Then the embedding chosen was not coherent with the definition, a contradiction.

For the cases of reflections at 30° and 60° the supposed robot r'_1 equivalent to r_1 , would lie outside the embedding of $mbp(F)$.

Regarding the case of a reflection at 90° , that is a reflection perpendicular to the X -axis, r_1 becomes equivalent to another robot r'_1 while moving toward its target. Now consider the other possible $bp'(F)$ having two sides parallel to the X -axis and shared with the chosen $bp(F)$. As in the case of a reflection at 0° , one side of $bp'(F)$ passes through r'_1 and the reading from this side

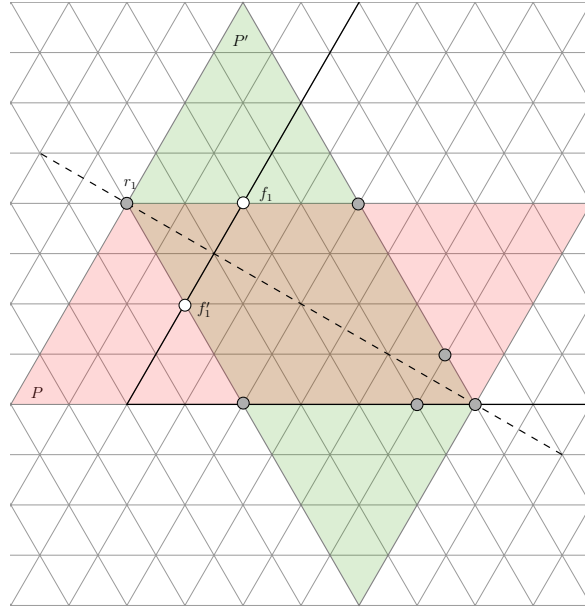


Fig. 11. Robot r_1 on a reflection axis of 30° and the equivalent parallelograms P and P' .

is lower than the reading of $bp(F)$ from the origin. Then the embedding chosen was not coherent with the definition, a contradiction.

Regarding the case of a reflection at 120° , the reflectional axis is parallel to the Y -axis, and r_1 becomes equivalent to another robot r'_1 while moving toward its target. The axis of symmetry must be between O and the half of the longest side of $bp(F)$. We now compare the reading of $bp(F)$ from O with the reading of $bp(F)$ starting from the corner at the opposite angle of 60° respect to O , call it P . The first column read from P has at most one robot, r'_1 equivalent to r_1 , then as many empty columns as those found from r_1 to the Y -axis in $mpb(R)$, until a first robot specular to the one read from O . Since the number of empty columns read from P is greater than the one read from O , the reading from P is lower than the reading from O hence a contradiction. In case of a reflection axis at 150° , the Y -axis reflects on the X -axis, then there is no possible robot r'_1 in the configuration that can be equivalent to r_1 when approaching to its target.

In what follows, we analyze the case when $R \setminus \{r_1\}$ forms an axis of symmetry.

Consider the case of a reflection at 0° . If the pattern is symmetric respect to that axis, f_1 is on the axis, and r_1 reaches the axis and proceeds along the axis without breaking the symmetry, by following the trajectory specified by move m_7 . If the pattern is asymmetric, then there are two possible embedding of F on $R \setminus \{r_1\}$ and then there must be another target f'_1 equivalent to f_1 obtained by reflecting the embedding such that the trajectory computed by the move of r_1 does not cross the axis (see Lemma 6). According to move m_7 , actually robot r_1 moves to f'_1 to finalize the task.

In case of a reflection axis of 30° , r_1 goes towards that axis and when it lands on it there two equivalent parallelograms $P = mpb(R)$ and its reflection P' . Let $l(P)$ and $l(P')$ the readings of the two parallelograms. These sequences are equivalent and they both find r_1 as the first robot. In each sequence r_1 is univocally determined and it can move respect to either P or P' toward

f_1 or f'_1 , respectively. As r_1 moves away from the axis, there is a unique $mbp(R)$ until r_1 reaches its target.

It is easy to see that when moving r_1 cannot go on an axis of 60° , 90° , and 120° before reaching its target.

Regarding to axes of 150° , r_1 could go on such an axis only if f_1 is under the reflection axis, but to be symmetric with such an axis the pattern should have the longest side laying on the Y -axis and this is not coherent with the embedding.

In conclusion, when moving r_1 does not create any rotation or reflection with a robot becoming equivalent to r_1 . The two cases in which r_1 creates a symmetric configuration is when it is on an horizontal axis and it moves along that axis or when is on a 30° axis and in this situation r_1 can always break the symmetry.

In order to conclude the proof of H_1 , we also need to ensure that r_1 is always recognized until reaching f_1 . In fact, as long as r_1 is sufficiently far away from the other robots it is easily recognizable according to its distance from O . When r_1 is close to the other robots is still always recognizable. In fact the parallelogram $mbp(R)$ is unique (apart from the case in which r_1 is on an axis of symmetry at 0° and 30°) and it can't be a square due the position of r_1 then there are two sequences of integers associated to the canonical corners of the $mbp(R)$. The minimal one finds r_1 as the first robot; in fact if there were another robot playing the role of r_1 in the minimal reading that reading would be a palindrome to the first sequence and that means that the configuration is symmetric. Since the algorithm doesn't create symmetric configurations, such palindrome reading cannot exist and then r_1 is unique. If r_1 lies on an axis, there are two parallelograms equivalent to $mbp(R)$ but the sequence of integers associated with these parallelograms finds r_1 as the first robot, then again r_1 is uniquely identified.

H_2 . During the movement of r_1 , predicate **qf1** remains true because $n-1$ robots are already matched, they all stay still and r_1 straightly moves towards its target along the direction of the longest side of $mbp(F)$. This implies that the sequence $\ell(mbp(R))$ keeps its structure given by the concatenation of a subsequence ℓ' made of only 0s and just one 1 in position d_{r_1} and a subsequence ℓ'_{f_1} that encodes the position of the robots already matched. When r_1 reaches its target $\ell(mbp(R)) = \ell(mbp(F))$ and the configuration is in T_8 .

H_3 . After each move, r_1 decreases the distance from f_1 while the sequence ℓ' gets smaller by a number of 0s equal to the shorter side of $mbp(R)$ until $\ell(mbp(R)) = \ell(mbp(F))$. This implies that within a finite number of LCM cycles **s** becomes true and C' belongs to T_8 . \square

Remark 6. We have shown that in fact algorithm \mathcal{A}_{form} manages not only asymmetric configurations but also some leader configurations where only one robot has to move and it is recognizable as one of the two guards r_1 or r_n .

Theorem 1 (Correctness). *Let $C = (G_T, \lambda)$ be any initial configuration with $n \geq 3$ ASYNC robots, and let F be any pattern (possibly with multiplicities) such that $|F| = n$. Then, \mathcal{A}_{form} is able to form F starting from C .*

Proof. What we are going to show is that if all properties H_1, \dots, H_3 hold, then for each possible execution of \mathcal{A}_{form} there exists a time t^* such that $C(t^*)$ is similar to F and $C(t) = C(t^*)$ for any time $t \geq t^*$. This implies that the statement holds.

Assume that C is provided as input to \mathcal{A}_{form} . According to properties **Prop**₁, \dots , **Prop**₃, there exists a single task (say T_i) to be assigned to robots with respect to C . According to H_1 , any configuration generated from T_i (say C') can be provided as input to \mathcal{A}_{form} . Moreover, by H_2 and H_3 , we can

consider C' belonging to some class (say T_j) different from T_i . According to this analysis, we can say that C' will evolve during the time by changing its membership from class to class according to the forward transitions defined by Lemmas 1–6. Although the execution of \mathcal{A}_{form} is infinite, property H_3 assures that any task is completed within a finite number of LCM cycles, apart for T_8 that will be reached within finite time t^* . Moreover, as the only movement allowed in T_8 is the *nil* one, then the reached configuration will not change anymore. \square

5 Extending the algorithm to graphs G_S and G_H

In this section, we briefly discuss how algorithm \mathcal{A}_{form} can be extended to solve the *APF* problem for asymmetric configurations defined on G_S or G_H .

The proposed algorithm uses few geometric concepts, such as: bounding parallelogram, grid line, shortest path, moving along a line, quadrant. Moving from G_T to G_S all these concepts remain valid, with the simplification that the canonical directions are reduced to two and consequently $bp(R)$ is unique. Moreover the moves do not need any changes and since predicates are independent from the underlying graph there is no need to change them. Hence the algorithm \mathcal{A}_{form} remains the same and the proof of its correctness still hold taking into consideration the necessary variations needed due the reduction of the canonical directions.

Moving to hexagonal grids, G_H is considered as a sub graph of G_T in which the center of the hexagons correspond to removed vertices. However by simply assuming the “presence” of the missing nodes and edges with respect to G_T , most of the geometric concepts introduced are still valid with the exception of “movement along a line”. In fact it cannot move along a line but it needs to move along the edges of successive hexagons. For instance, in tasks T_1 and T_2 , \mathcal{A}_{form} simply requires that r_1 reaches the target via shortest paths, without assuming other constraints. So, even in G_H the moves m_1 and m_2 remain valid. Conversely, during T_3 r_n moves along the Y -axis according to \mathcal{A}_{form} . In this case we need to specify how the move unfolds since there are missing edges respect to G_T . In the following paragraph we revise the algorithm and give the details of the changes needed in order to extend \mathcal{A}_{form} for hexagonal grids.

5.1 Hexagonal grid graphs

G_H is considered as a sub graph of G_T in which the center of the hexagons correspond to removed vertices. The basics concepts defined for G_T naturally extend to G_H . In particular:

- the distance function between two vertices u and v in G_H is the length of a shortest path connecting u and v in G_T ;
- canonical directions in G_H are the directions of the edges incident to a single vertex, the same introduced in G_T . Given the canonical directions, we consider the same definition for an *mpb* as in G_T . Given a vertex v and oriented line L passing through v toward a canonical direction, vertex v can be classified in one of these three types:
 - type 0: if v is not in G_H ;
 - type 1: if v has an edge following the orientation of L ;
 - type 2 otherwise.

The type of a leading corner is determined by the reading in the same direction that originates the sequence of $mbp(F)$.

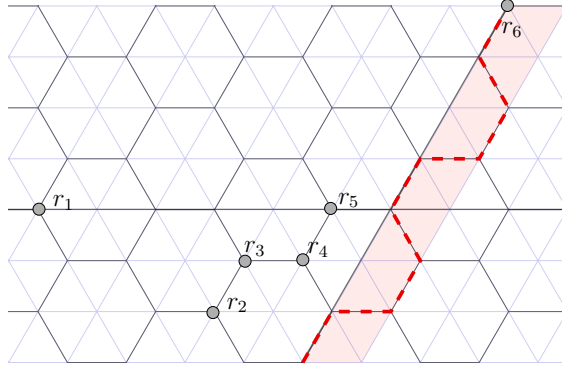


Fig. 12. Robot r_6 moving in a band during task T_3 .

- the sequence of integers associated to a configuration of robots is the same as defined for G_T placing a zero in the sequence in correspondence of a vertex in G_T but not in G_H .

Further concepts will be introduced in the following description of the algorithm. In the hexagonal graph, to go toward a direction, a robot either moves to the adjacent vertex if there is an edge connecting the two or it moves along the edges of the next hexagon ahead. Therefore a robot moves alternatively straight or diverting its path. As a result, the movement of a robot is enclosed in a band that is tall half the height of an hexagon while moving toward a direction. Given a robot and three canonical directions, there are two bands for each direction, the band selected each time by the robot is specified in a task when needed.

- Task T_1 : During this task robot r_1 moves away from the other robots until predicate **g1** becomes true. For hexagonal grids predicate **g1** is updated as follows:
g1 : r_1 is at a vertex such that exists a unique direction in which at least one of the lines passing through r_1 or one of its neighbours encounters each $bp(R')$.
- Task T_2 : In this task r_1 moves at a distance 3Δ from the origin. The origin here is redefined since it can be a vertex of G_T not in G_H . Given r_1 and r_n , let R'' be $R'' = R \setminus \{r_1, r_n\}$. Let L be the line that forms a canonical angle with X passing through a robot in R'' and farthest from r_1 . The origin is defined as the first vertex encountered from the intersection of L and X having the same type of the leading corner of $mbp(F)$ read following the orientation of the Y-axis.
- Task T_3 : In this task r_n moves toward its target through any shortest path while keeping outside $mpb(R'')$ also during a detour.
- Task T_4 : In this task $n - 2$ robots reach their target one by one. This task develops in the same way as in G_T .
- Task T_5 : In this task guard r_n goes towards its target f_n . While moving parallel to the X-axis, r_n moves in any band that keeps at least 2Δ distance from X . While moving parallel to the Y-axis, r_n moves in the band farthest from r_1 . Predicate **hrn** is updated as follows:
hrn : $f_n = (x, y)$ and $r_n = (x', y')$, with $x' \leq x + 1$ and $y' \geq y$
- Task T_6 : In this phase r_1 moves parallel to the shortest side of the parallelogram $mbp(R)$ as to increase d_r . During the movement r_1 moves in any band that keeps at least $3w(mbpf(F))$ distance from $mbp(F)$. We say that r_1 is in line with its target if $d_r = d_f$ or $d_r - 1 = d_f$ since r_1 is moving within a band, so predicate **qf1** updates as follows:

- qf1 : $\ell(\text{mbp}(R)) = \ell' + \ell_{f_i}^F$, for some ℓ' made of only 0's and just one 1 in position d_r and $(d_r = d_f \vee d_r - 1 = d_f)$.
- Task T_7 : In this task r_1 moves towards its target and in case of detours it moves in the direction such that $\ell(\text{mbp}(R))$ decreases.

The same proofs of correctness given in Section 4.2 for G_T apply for G_H .

6 Conclusion

One may ask why in regular tessellation graphs *APF* does not show the same solvability properties of the case of robots moving in the Euclidean plane. There, in fact, any leader configuration can be taken in input with the idea that it is always possible to break the possible symmetry by moving the leader. Here, in graphs, this strategy does not seem to be effective as the movements of the robots are restricted to the neighborhood. Hence, in a symmetric leader configuration it may happen the leader cannot move without causing a multiplicity which might prevent the formation of the final pattern (e.g., consider the case of a rotational configuration defined on G_S with a robot on the center of rotation and all its four neighbors occupied). Hence, before moving the leader, a resolution strategy should make “enough space” around the leader. Actually, this approach has been followed in [5], a very recent work. In that paper, an algorithm able to break symmetries in leader configurations defined on G_S or G_T has been proposed. As a natural possible future work, it would be interesting to check whether this breaking symmetry algorithm can be composed with \mathcal{A}_{form} . If possible, this would completely solve the *APF* problem on both G_S and G_T .

References

1. Bhagat, S., Chaudhuri, S.G., Mukhopadhyaya, K.: Formation of general position by asynchronous mobile robots under one-axis agreement. In: Proc. 10th Int.'l WS on Algorithms and Computation (WALCOM). LNCS, vol. 9627, pp. 80–91. Springer (2016)
2. Bose, K., Adhikary, R., Kundu, M.K., Sau, B.: Arbitrary pattern formation on infinite grid by asynchronous oblivious robots. In: Proc. 13th Int.'l Conf. on Algorithms and Computation (WALCOM). LNCS, vol. 11355, pp. 354–366. Springer (2019)
3. Bose, K., Adhikary, R., Kundu, M.K., Sau, B.: Arbitrary pattern formation by opaque fat robots with lights. In: Proc. 6th Int.'l Conf. on Algorithms and Discrete Applied Mathematics (CALDAM). LNCS, vol. 12016, pp. 347–359. Springer (2020)
4. Bramas, Q., Tixeuil, S.: Arbitrary pattern formation with four robots. In: Proc. 20th Int.'l Symp. on Stabilization, Safety, and Security of Distributed Systems (SSS). LNCS, vol. 11201, pp. 333–348. Springer (2018)
5. Cicerone, S.: Breaking symmetries on tessellation graphs via asynchronous robots. In: Cordasco, G., Gargano, L., Rescigno, A. (eds.) Proceedings of the 21st Italian Conference on Theoretical Computer Science (ICTCS), 2020. CEUR Workshop Proceedings, CEUR-WS.org (2020), to appear
6. Cicerone, S., Di Stefano, G., Navarra, A.: Gathering of robots on meeting-points: feasibility and optimal resolution algorithms. Distributed Computing **31**(1), 1–50 (2018)
7. Cicerone, S., Di Stefano, G., Navarra, A.: “Semi-Asynchronous”: a new scheduler for robot based computing systems. In: Proc. 38th IEEE Int.'l Conf. on Distributed Computing Systems, (ICDCS). pp. 176–187. IEEE (2018)
8. Cicerone, S., Di Stefano, G., Navarra, A.: Asynchronous arbitrary pattern formation: the effects of a rigorous approach. Distributed Computing **32**(2), 91–132 (2019)

9. Cicerone, S., Di Stefano, G., Navarra, A.: Embedded pattern formation by asynchronous robots without chirality. *Distributed Computing* **32**(4), 291–315 (2019)
10. Cicerone, S., Di Stefano, G., Navarra, A.: A methodology to design distributed algorithms for mobile entities: the pattern formation problem as case study. *CoRR* **abs/2010.12463** (2020), <https://arxiv.org/abs/2010.12463>
11. Cieliebak, M., Flocchini, P., Prencipe, G., Santoro, N.: Distributed computing by mobile robots: Gathering. *SIAM J. on Computing* **41**(4), 829–879 (2012)
12. D’Angelo, G., Di Stefano, G., Klasing, R., Navarra, A.: Gathering of robots on anonymous grids and trees without multiplicity detection. *Theor. Comput. Sci.* **610**, 158–168 (2016)
13. Das, S., Flocchini, P., Prencipe, G., Santoro, N., Yamashita, M.: Autonomous mobile robots with lights. *Theor. Comput. Sci.* **609**, 171–184 (2016)
14. Das, S., Flocchini, P., Santoro, N., Yamashita, M.: Forming sequences of geometric patterns with oblivious mobile robots. *Distributed Computing* **28**(2), 131–145 (2015)
15. D’Emidio, M., Di Stefano, G., Frigioni, D., Navarra, A.: Characterizing the computational power of mobile robots on graphs and implications for the euclidean plane. *Inf. Comput.* **263**, 57–74 (2018)
16. Di Stefano, G., Navarra, A.: Gathering of oblivious robots on infinite grids with minimum traveled distance. *Inf. Comput.* **254**, 377–391 (2017)
17. Dieudonné, Y., Petit, F., Villain, V.: Leader election problem versus pattern formation problem. In: *Proc. 24th Int.’l Symp. on Distributed Computing (DISC)*. LNCS, vol. 6343, pp. 267–281. Springer (2010)
18. Flocchini, P., Prencipe, G., Santoro, N., Widmayer, P.: Gathering of asynchronous robots with limited visibility. *Theor. Comput. Sci.* **337**, 147–168 (2005)
19. Flocchini, P., Prencipe, G., Santoro, N., Widmayer, P.: Arbitrary pattern formation by asynchronous, anonymous, oblivious robots. *Theor. Comput. Sci.* **407**(1-3), 412–447 (2008)
20. Ghike, S., Mukhopadhyaya, K.: A distributed algorithm for pattern formation by autonomous robots, with no agreement on coordinate compass. In: *Proc. 6th Int.’l Conf. on Distributed Computing and Internet Technology, (ICDCIT)*. LNCS, vol. 5966, pp. 157–169. Springer (2010)
21. Grünbaum, B., Shepard, G.C.: *Tiling and Patterns*. W. H. Freeman & Co., New York (1987)
22. Ionascu, E.J.: Half domination arrangements in regular and semi-regular tessellation type graphs. *Math* **abs/1201.4624v1** (2012), <https://arxiv.org/abs/1201.4624v1>
23. Suzuki, I., Yamashita, M.: Distributed anonymous mobile robots: Formation of geometric patterns. *SIAM J. Comput.* **28**(4), 1347–1363 (1999)
24. Yamashita, M., Suzuki, I.: Characterizing geometric patterns formable by oblivious anonymous mobile robots. *Theor. Comput. Sci.* **411**(26-28), 2433–2453 (2010)
25. Yamauchi, Y., Uehara, T., Kijima, S., Yamashita, M.: Plane formation by synchronous mobile robots in the three dimensional euclidean space. In: *Proc. 29th Int.’l Symp. on Distributed Computing (DISC)*. LNCS, vol. 9363, pp. 92–106. Springer (2015)
26. Yamauchi, Y., Yamashita, M.: Randomized pattern formation algorithm for asynchronous oblivious mobile robots. In: *Proc. 28th Int.’l Symp. on Distributed Computing, (DISC)*. LNCS, vol. 8784, pp. 137–151. Springer (2014)